INTERNATIONAL JOURNAL OF REFRIGERATION 74 (2017) 642–648

Available online at www.sciencedirect.com

ScienceDirect

journal homepage: www.elsevier.com/locate/ijrefrig

An apparatus to measure the thermal conductivity of insulation panels at sub-ambient temperature

S. Vanapalli *, *T. Klünder*, *I. Hegeman*, *N. Tolboom*, *H.J.M. ter Brake*

University of Twente, P.O.B 217, 7500 AE Enschede, The Netherlands

ARTICLE INFO

Article history:
Received 10 June 2016
Received in revised form 24 November 2016
Accepted 27 November 2016
Available online 8 December 2016

Keywords:
Vacuum insulation panel
Thermal conductivity
Guard heater
Passive container

ABSTRACT

A single-sided guarded-plate apparatus has been developed to measure the thermal conductivity of insulation panels of sub-meter size at sub-ambient temperatures ranging from 250 to 300 K. This apparatus allows thermal conductivity measurements to be performed at large temperature differences simulating the actual operating conditions in an application and can accommodate panels of various thickness. The cold plate in the apparatus is cooled with a flow thermostat. The reduction in performance due to the heat conductance along the edge of a vacuum insulation panel is significant at small panel sizes and is detrimental to the end application. The effective thermal conductivity of square vacuum insulation panels of several thickness and area is measured, and is observed that the square panels of side 10 and 20 cm have about twice higher thermal conductivity than their larger counterparts due to the heat leak along the edges of these panels.

Un appareil pour mesurer la conductivité thermique de panneaux d'isolation à une température sous-ambiante

Mots clés : Panneau d'isolation sous vide ; Conductivité thermique ; Réchauffeur à barrière de protection ; Conteneur passif

1. Introduction

Technologies to enable small-scale efficient passive transportation of refrigerated products is gaining importance due to the increasing need to ship products such as food, biological materials, pharmaceuticals, medicines, blood and many more (Elliott and Halbert, 2005; Hyde et al., 2015; Morris, 1996; Rentas et al., 2004). Typically, a passive cold container uses a phase change material (Oro et al., 2012; Veerakumar and Sreekumar, 2016) and a high performance thermal insulation. The phase change material is regenerated in a standalone refrigerator

* *Corresponding author.* University of Twente, P.O.B 217, 7500 AE Enschede, The Netherlands. Fax: +31 53 4891099.
E-mail address: s.vanapalli@utwente.nl (S. Vanapalli).
http://dx.doi.org/10.1016/j.ijrefrig.2016.11.022
0140-7007/

Nomenclature

A	area [m^2]
I	current [A]
L	latent heat [J kg^{-1}]
$\dot{m}$	mass flow rate [kg s^{-1}]
p	perimeter [m]
P	electrical power [W]
$\dot{Q}$	heat flow [W]
R	thermal resistance [K W^{-1}]
T	temperature [K]
t	length, perpendicular to area A [m]
U	thermal conductance [W K^{-1}]
V	voltage [V]

Greek symbols

λ	thermal conductivity [W m^{-1} K^{-1}]

Subscripts

ambient	surrounding
c	sub-ambient
clamp	clamping structures
contact	contact between two surfaces
core	center of the panel
edge	sides of the panel
eff	effective
leads	electrical leads
radiation	thermal radiation
rest-gas	residual gas

before every use. Vacuum insulation panels are increasingly used in these containers because of superior insulating characteristics (Fricke et al., 2006; Hammond and Evans, 2014). Commercially available vacuum insulation panels are specified with an effective thermal conductivity value of less than 5 mW m^{-1} K^{-1} (Fricke et al., 2008).

A vacuum insulation panel is made of fumed silica as the core material, which is evacuated to a pressure lower than 1 mbar. The core is enclosed in an envelop of high-barrier (for air and moisture) laminate, which consists of several layers of Al-coated polyethylene (PE) and polyethylene terephthalate (PET). Wakili et al. (2004) investigated the thermal conductance at the contact of the laminate along the edge of the panel, termed as thermal bridging effect and suggested that this effect cannot be neglected. Experiments performed by these authors show that thermal conductivity due to the edge effect is about 11% of the effective thermal conductivity, for a panel with an area of 1 m^2 and a thickness of 2 cm. The measured effective thermal conductivity of this panel is 4.70 mW m^{-1} K^{-1} with hot and cold sides at 15 °C and 5 °C, respectively. The edge effect scales with the perimeter of the panel. Therefore, the insulation characteristics of small panels are likely to be poor compared to their larger counterparts.

The main objective of this paper, is to design an apparatus that can accurately measure the thermal conductivity of square panels of side in the range of 10–20 cm, in the sub-ambient temperature range. A single-sided guarded-heater apparatus is developed that allows specimens of various heights to be tested. Experiments are performed in a vacuum environment to reduce the parasitic heat leaks.

In this paper, a brief review of the experimental methods to perform sub-ambient thermal conductivity measurements is presented. This review is limited to suitable techniques for characterization of flat insulation panels. A single-sided guarded heater apparatus is described, followed by the measurement results. Various sizes of commercially available vacuum insulation panels are characterized.

2. Measurement methods

In this section, a review of experimental methods used to determine the effective thermal conductivity of insulation panels is described. It is important to note that this review is restricted to methods where flat panels can be accommodated.

The essence of any steady state thermal conductivity apparatus is based on the Fourier's law of heat conduction,

$$\dot{Q} = \lambda A \vec{\nabla} T \tag{1}$$

where $\dot{Q}$ is heat flow, A is the area, and T is the temperature. The thermal conductivity λ is determined by setting a temperature difference across the panel and measuring the heat flow through the panel. Assuming a one-dimensional heat flow along a thickness t of the panel, the thermal resistance R (and reciprocal, conductance U) of the panel is,

$$R \equiv \frac{\Delta T}{\dot{Q}} = \frac{t}{\lambda A} \quad \text{and} \quad U = R^{-1}. \tag{2}$$

In reality depending on the construction and operational parameters of the test rig several parasitic heat flows should be considered. Fig. 1 shows a thermal resistance network of a generalized thermal conductivity measurement apparatus. Here, the hot plate is controlled at ambient temperature $T_{ambient}$ and the cold plate is at sub-ambient temperature T_c. The resistance of the panel $R_{specimen}$ is the parameter of interest in these measurements. The other resistances are summarized below:

- $R_{contact}$: The contact resistance between the panel and the hot/cold plate.
- R_{clamp} : The clamping structures contribute to heat flow between the hot and cold plates.
- $R_{radiation}$: Thermal radiation from the ambient on the cold parts.
- $R_{rest-gas}$: Heat flow from air surrounding the specimen.
- R_{leads} : Heat conduction through the wiring of the sensors.

It is important to note here that the heat conduction through the sensor/heater wires to the hot plate is not considered because the hot plate temperature is set to ambient temperature.

A schematic of relevant measurement apparatus to determine the thermal conductivity of insulation panels is shown in Fig. 2. These methods are briefly visited below.

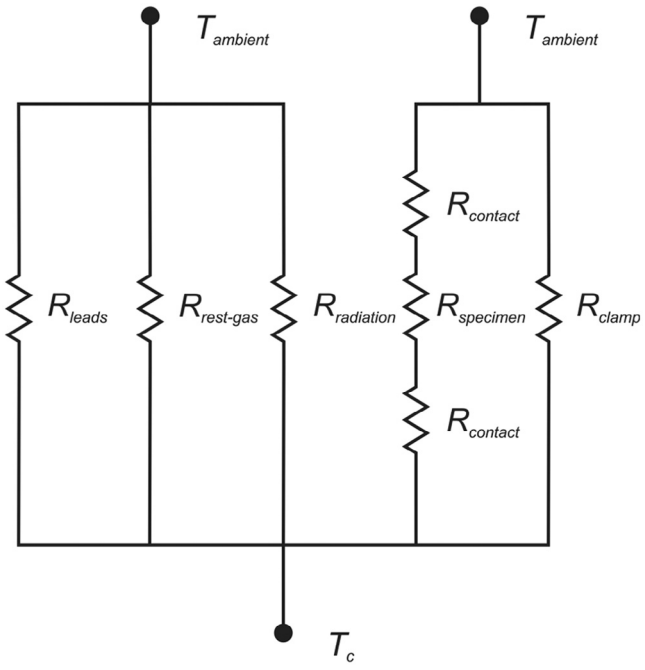

Fig. 1 – The thermal network of a generalized thermal conductivity measurement apparatus representing various thermal resistances between the hot plate $T_{ambient}$ and the cold plate T_c temperatures.

2.1. *Boil-off calorimetry*

Boil-off calorimetry is a technique often used to measure the thermal conductivity of insulation materials around cryogenic temperature (Powell et al., 1957). One side of the specimen is set to a fixed temperature and the other side is brought in contact with a cryogenic liquid. The heat flow through the insulation panel causes the cryogenic liquid to boil. The vaporized mass flow $\dot{m}$ is measured and the heat flow is given by $\dot{Q} = \dot{m} \cdot L$, where L is the latent heat of vaporization of the fluid. A major drawback of this method is a fixed cold-plate temperature (the boiling point of the cryogenic fluid). Moreover, a reference calibration of the system should be performed before measurement of the sample to account for parasitic heat leaks to the cold plate. The accuracy of thermal conductivity depends on the accuracy of mass flow measurement. In case of small sample size as proposed in this paper, the flow rate is rather small to measure and therefore this method is not suitable.

2.2. *Guarded hot-plate method*

In this method, the hot plate is sandwiched between a pair of insulation panels (Wakili et al., 2004). Each insulation panel is enclosed by a cold plate (see Fig. 2). The dimensions of each panel should be precisely measured. The heat flow to the hot plate is measured and an effective thermal conductivity of both the panels is determined. This method is often used to characterize insulation panels around room temperature. At sub-ambient cold plate temperature the test rig gets very complex due to two cold plates. Another disadvantage of this method is the requirement of two identical specimens in each measurement, which is rather challenging for small specimen sizes.

2.3. *Single-sided guarded-hot-plate method*

In this method a single guard heater is used (see Fig. 2). This method is used to characterize spray-on foam insulation at cryogenic temperature (Barrios and Van Sciver, 2013). In their measurements, the temperature difference between the hot and cold plate is set to 20 K. The design of the apparatus described in this paper draws inspiration from their test rig. The main differences are:

- The hot plate and the guard heater are always controlled at ambient temperature, which eliminates the heat leak due to sensor leads.
- The insulation panels height can be varied.
- The thermal conductivity of the insulation panel can be measured with the actual temperature difference experienced in an application (ambient on one side and sub-ambient on the other side) due to the use of coolant in the cold plate.

3. Test rig

3.1. *Set-up*

The apparatus described in this paper is similar to the guidelines described in the ASTM standard C177, “Standard Test Method for Steady-State Heat Flux Measurements and Thermal

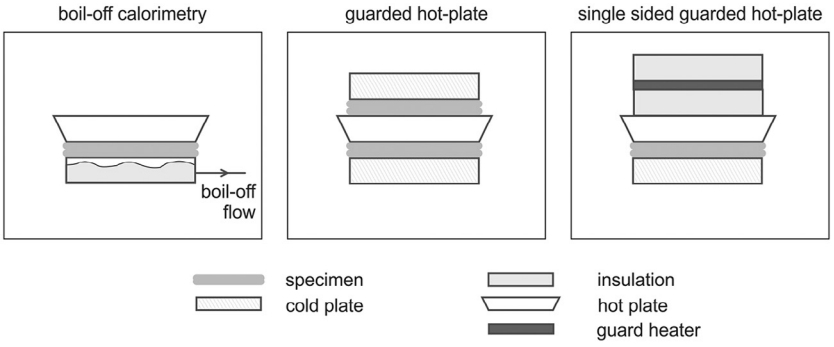

Fig. 2 – Overview of suitable experimental methods to measure the thermal conductivity of insulation panels.

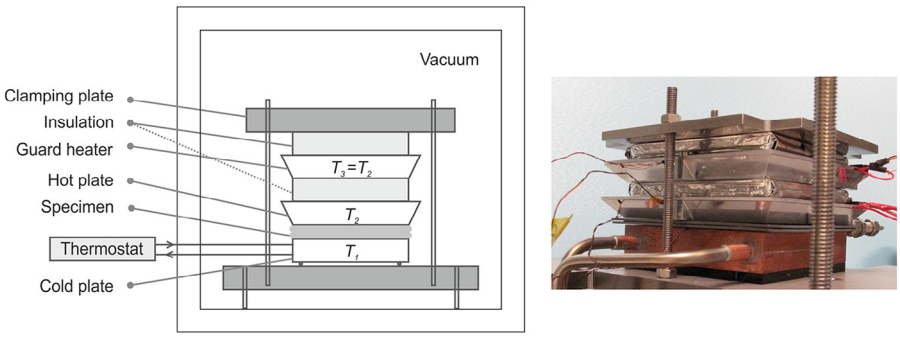

Fig. 3 – (*Left*) A schematic of the single-sided guarded hot-plate apparatus. (*Right*) Photo of the assembled stack of cold plate, specimen, hot plate, insulation, guard heater, insulation and clamping plate.

Transmission Properties by Means of the Guarded-Hot-Plate Apparatus", with changes to accommodate the additional requirements to operate at sub-ambient temperature. Fig. 3 shows the schematic of the test rig with a guard heater, hot plate, specimen, and a cold plate. The base is made of stainless steel plate. The cold plate consists of a copper block with embedded channels for the flow of a coolant. The temperature of the coolant is regulated with a Julabo FP89 thermostat bath, which is located outside the vacuum jar. On the cold plate the specimen is mounted. The hot plate is made of two aluminium plates with a kapton heater sandwiched between them. Due to the good thermal conductance of aluminium, heat is uniformly distributed along the entire area of the hot plate.

On the hot plate, an insulation panel and a guard heater are mounted. The guard plate heater is controlled such that the guard plate has the same temperature as the hot plate. An insulation panel and a clamping plate are mounted on the guard plate. The clamping plate is fixed to the base plate with four stainless steel threaded rods to apply force on the entire stack.

On both sides of the insulation panel, vacuum grease (ApiezonN) is smeared to minimize the contact resistance. The vacuum grease has a thermal conductance of 1 W K^{-1} for a layer thickness of 10 μm, which is rather high compared to the expected thermal conductance of the insulation panels (~mW K^{-1}). Temperature sensors are mounted at the center of the cold plate, hot plate and the guard heater. The electrical leads to the sensors and the heater cause parasitic heat leak to/from the ambient. Since all the heaters are maintained at ambient temperature, the heat leak from the leads is zero. However, this is not the case for the sensors located in the cold plate. The cooling capacity of the thermostat is about 200 W at 230 K. A copper lead of 1 m length and a diameter of 0.8 mm causes a heat leak of 12 mW with a temperature difference of 60 K. A maximum heating power of 2 W is used in the hot plate in the experiments. Therefore, the parasitic heat leak due to leads located in the cold plate is not an issue.

The heat leak due to the conduction to the ambient gas is minimized by performing the experiments in vacuum. A vacuum pressure less than 1 Pa is maintained. The heater is wrapped with multi-layer insulation to reduce the radiation heat load to the cold plate.

3.2. *Measurement uncertainty analysis*

The uncertainty in the thermal conductivity of insulation panels is determined from the measured parameters and is discussed in this section. Lakeshore 670 series diode thermometers are used and the uncertainty specified by the supplier is $\delta T = 0.5$ K. The self-heating of the diode thermometers is 1 μW, which is relatively small compared to the heat flow from the hot to cold plates and is neglected. The voltage over and the current through the kapton heaters are measured using a 4-point method. The error in the measurement of current and voltage is $\delta I = 0.05$ A and $\delta V = 0.1$ V, respectively. The error of the data acquisition card is 0.2 mV over the full scale range from –10 to 10 V, which is small relative to the measured voltage and is neglected.

The heating power is calculated by multiplying the voltage V over and the current I through the heater. The uncertainty in the power is obtained as,

$$\delta P = |P| * \left[\left(\frac{\delta V}{|V|} \right)^2 + \left(\frac{\delta I}{|I|} \right)^2 \right]^{1/2}. \tag{3}$$

The error in temperature difference is the sum of the errors of the sensors at the hot and cold plates, which is equal to $\delta \Delta T = 1.0$ K. The uncertainty of thermal conductivity is,

$$\delta \lambda = |\lambda| * \left[\left(\frac{\delta V}{|V|} \right)^2 + \left(\frac{\delta I}{|I|} \right)^2 + \left(\frac{\delta \Delta T}{|\Delta T|} \right)^2 \right]^{1/2}. \tag{4}$$

4. Results and discussion

The nominal dimensions of the panels considered in this paper are shown in Table 1. Vacuum insulation panels from two suppliers (vaQtec and Promat) are measured. Fig. 4 shows measurement data for three sizes of vaQtec panels. The top row of the plots in this figure show the heating power as a function of temperature difference between the hot and cold plates. The hot plate is controlled at ambient temperature of 293 K.

Table 1 – Data of all the types of vacuum insulation panels considered in this paper.

Source	Nominal dimensions (mm)	Effective thermal conductivity (mW m^{-1} K^{-1})	Effective thermal conductance (mW K^{-1})
vaQtec	100 × 100 × 10	11.4 ± 0.4	11.2
vaQtec	100 × 100 × 20	8.7 ± 0.2	4.6
vaQtec	200 × 200 × 10	8.5 ± 0.4	32.7
Promat	100 × 100 × 10	11.6 ± 0.1	11.8
Promat	200 × 200 × 30	11.0 ± 0.6	13.7

The experiments are performed in a temperature controlled laboratory where the ambient temperature variation is less than 2 °C. A least square linear fit of the data is also shown in the plots. The intercept of these fits is set to zero, so as to represent the physical system under consideration. The slope of the fit is a measure of the average thermal conductance. Table 1 lists the average thermal conductance of the measured panels.

The lower plots in Fig. 4 show the thermal conductivity determined from the measured power, temperature difference and dimensions of each panel using Eq. (2). Similar plots are shown for Promat panels in Fig. 5. For all the panels

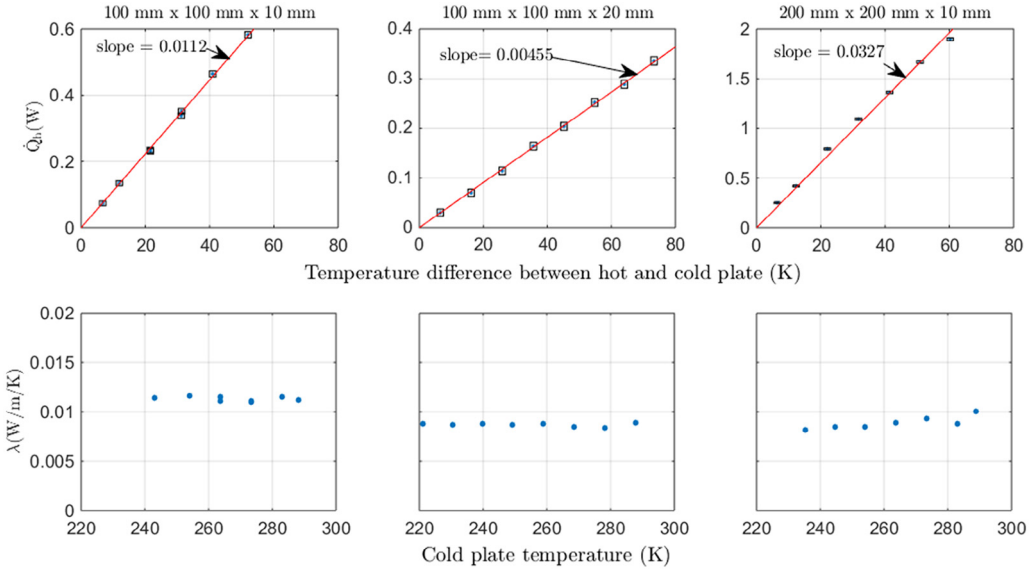

Fig. 4 – Measurement data of vaQtec supplied panels.

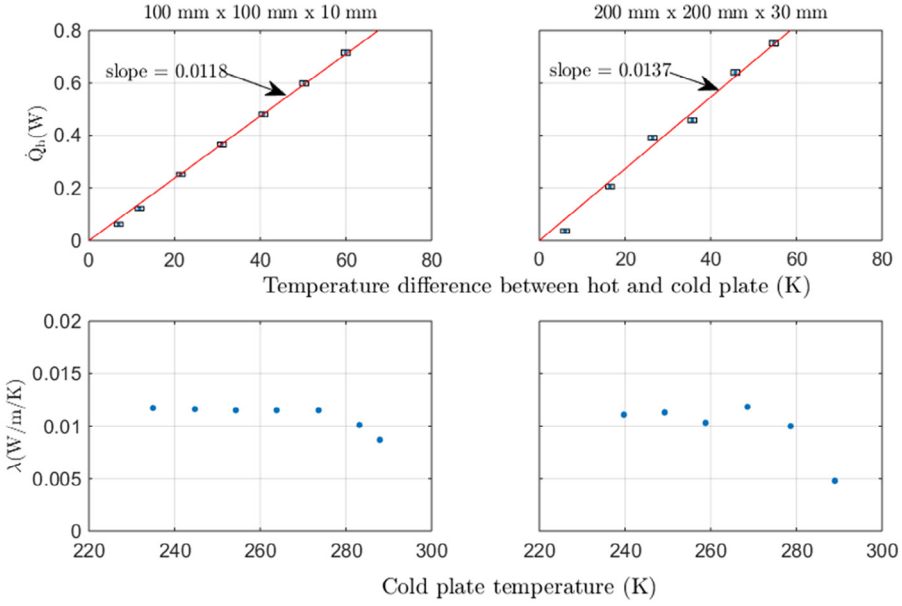

Fig. 5 – Measurement data of Promat supplied panels.

considered in this study, it is observed that the thermal conductivity does not vary with the cold-plate temperature within the measurement range. The variation of thermal conductivity as observed in plots close to room temperature is due to inaccuracy of the thermometers, since the temperature difference used in determining thermal conductivity is small.

The effective thermal conductivity shown in Table 1 is determined from the effective thermal conductance using Eq. (2). In order to apply this equation, the dimensions of the panel are required. We noticed slight differences in the dimensions of the actual measured values and the nominal values specified by the supplier. The measured values are shown in the Appendix. The uncertainty of the thermal conductivity shown in Table 1 is determined from the statistical error in the slope of the fit to the heat vs temperature difference plots and the error in dimensions compared to the nominal value.

The specification of effective thermal conductivity for the panels considered in this study is less than 5 mW m^{-1} K^{-1}. However, the measured values are much larger than the specified value, in three cases the difference is more than twice (see Table 1). Our hypothesis is that the difference could be due to the thermal bridging of the foil at the edges of the panels. Wakili et al. (2004) proposed an expression for the effective thermal conductivity of vacuum insulation panel, as a sum of thermal conductivity of the core and the edge of the panel.

$$\lambda_{eff} = \lambda_{core} + \lambda_{edge} = \lambda_{core} + \psi(d) \times d \times p/A \quad (5)$$

The parameter $\psi(d)$ is the linear thermal transmittance of the panel, which depends on the panel thickness and should be experimentally determined. In this study, to separate the core and edge effects, a thermal network model of a panel is used. The panel can be represented by two parallel thermal resistances, one resistance represents the core of the panel and the second resistance the edge effect (see Table 2). Let us benchmark these resistances by considering a 100 mm × 100 mm × 10 mm panel. The core resistance in this case is R_{core} and the edge resistance is R_{edge}. A panel with dimensions 100 mm × 100 mm × 20 mm will have a core resistance equal to $2 \cdot R_{core}$ and edge resistance of R_{edge}. The edge resistance remains the same because the thermal path is along the contact between the two foils at the edge of the panel, which is independent of the thickness of the panel. By using the experimentally determined effective conductance of these two panels shown in Table 1, the core conductance (reciprocal of resistance) U_{core} is 5.4 mW K^{-1} and the edge conductance U_{edge} is 6.0 mW K^{-1}. Using these values, the effective resistance of the 200 mm by × 200 mm × 10 mm panel can be predicted. The equivalent thermal resistance of this panel is shown in Table 2. The estimated thermal conductance is 33.6 mW K^{-1} and the corresponding thermal conductivity is 8.4 mW m^{-1} K^{-1}, which agrees well with the measured value of 8.5 ± 0.4 mW m^{-1} K^{-1} (see Table 1). This proves the hypothesis that edge effects are the reason for larger thermal conductivity values of relatively small vacuum insulation panels.

Table 2 – Effective resistance of the panels.

Nominal dimensions (mm)	Core resistance	Edge resistance	Effective resistance
100 × 100 × 10	R_{core}	R_{edge}	$\frac{R_{core}R_{edge}}{R_{core}+R_{edge}}$
100 × 100 × 20	$2 \cdot R_{core}$	R_{edge}	$\frac{2 \cdot R_{core}R_{edge}}{2 \cdot R_{core}+R_{edge}}$
200 × 200 × 10	$R_{core}/4$	$R_{edge}/2$	$\frac{R_{core}R_{edge}}{2(R_{core}+2 \cdot R_{edge})}$

The higher values of effective thermal conductivity of small panels compared to their larger counterparts will have direct implications to the design of a small-scale (shoebox sized) transportation container. To achieve sufficiently lower thermal conductance and therefore longer transit time, thicker panels should be used, which will increase the weight of the container. Therefore a trade-off between the size (volume), weight and performance (transit time) of the container should be considered.

5. Conclusions

We developed a single-sided guard heater apparatus to measure the thermal conductivity of sub-meter sized insulation panels at sub-ambient temperature. The cold plate temperature is controlled by a flow thermostat. The hot plate is maintained at ambient temperature to simulate realistic test conditions and more over to cancel the parasitic heat leaks due to conduction of the sensor/heater leads and radiation from ambient. The tests indicate that the edge effect of the vacuum insulation panels is significant at sizes 100–200 mm. The effective thermal conductivity of a 100 mm × 100 mm × 10 mm panel is about 11 mW m^{-1} K^{-1}, which is more than twice higher compared to a meter sized panel. Therefore while designing a shoebox size passive transportation container with vacuum insulation panels, the edge effect cannot be neglected.

Acknowledgement

The authors acknowledge lab assistance of Cris Vermeer and Harry Holland.

Appendix

Dimensions of the vacuum insulation panels

We noticed differences in dimensions of the each panel when measured at several locations. Since the calculation of thermal conductivity (Eq. (2)) requires dimensions of the panel, measurements were performed at various locations and an average value is determined (shown in bold face in the table below). The length and the width of the panel is measured on each side and in the middle on top and bottom side of each panel (six readings). The thickness is measured at all the four corners.

vaQtec 100 mm × 100 mm × 10 mm panel							
Length (mm)	100.6	100.7	100.6	101.3	101.3	101.0	**100.9**
Width (mm)	98.8	99.5	99.2	100.3	99.9	100.4	**99.7**
Thickness (mm)	10.3	10.4	10.0	10.4			**10.3**
vaQtec 100 mm × 100 mm × 20 mm panel							
Length (mm)	100.9	101.6	100.8	100.6	100.6	100.7	**100.9**
Width (mm)	100.1	100.5	100.6	100.6	100.2	100.1	**100.3**
Thickness (mm)	19.3	19.2	19.9	19.4			**19.4**
vaQtec 200 mm × 200 mm × 10 mm panel							
Length (mm)	201.1	200.3	201.8	199.8	199.1	200.4	**200.4**
Width (mm)	200.0	199.7	199.7	198.9	199.8	198.9	**199.5**
Thickness (mm)	10.2	10.2	10.5	10.4			**10.4**
Promat 100 mm × 100 mm × 10 mm panel							
Length (mm)	96.2	97.9	98.4	98.3	97.6	97.7	**97.7**
Width (mm)	96.3	96.7	97.7	98.2	97.3	96.9	**97.4**
Thickness (mm)	8.8	9.4	9.8	9.3			**9.3**
Promat 200 mm × 200 mm × 30 mm panel							
Length (mm)	197.8	197.7	197.9	196.8	196.7	196.5	**197.2**
Width (mm)	198.9	198.9	199.0	197.4	197.8	197.4	**198.2**
Thickness (mm)	28.4	28.7	28.6	29.5			**28.8**

REFERENCES

Barrios, M., Van Sciver, S., 2013. Thermal conductivity of rigid foam insulations for aerospace vehicles. Cryogenics 55, 12–19.

Elliott, M., Halbert, G., 2005. Maintaining the cold chain shipping environment for Phase I clinical trial distribution. Int. J. Pharm. 299, 49–54.

Fricke, J., Schwab, H., Heinemann, U., 2006. Vacuum insulation panels – exciting thermal properties and most challenging applications. Int. J. Thermophys. 27, 1123–1139.

Fricke, J., Heinemann, U., Ebert, H., 2008. Vacuum insulation panels – from research to market. Vacuum 82, 680–690.

Hammond, E., Evans, J., 2014. Application of vacuum insulation panels in the cold chain–analysis of viability. Int. J. Refrigeration 47, 58–65.

Hyde, R.A., Jung, E.K., Myhrvold, N.P., Tegreene, C.T., Gates, W., Whitmer, C., et al., Temperature-stabilized medicinal storage systems, 2015. US Patent 9,138,295.

Morris, R., Portable cooling container, 1996. US Patent 5,490,396.

Oro, E., Miro, L., Farid, M.M., Cabeza, L.F., 2012. Thermal analysis of a low temperature storage unit using phase change materials without refrigeration system. Int. J. Refrig. 35, 1709–1714.

Powell, R.L., Rogers, W.M., Coffin, D.O., 1957. An apparatus for measurement of thermal conductivity of solids at low temperatures. Bur. Stand. J. Res. 59, 349–355.

Rentas, F.J., Macdonald, V.W., Houchens, D.M., Hmel, P.J., Reid, T.J., 2004. New insulation technology provides next-generation containers for iceless and lightweight transport of RBCs at 1 to 10°C in extreme temperatures for over 78 hours. Transfusion 44, 210–216.

Veerakumar, C., Sreekumar, A., 2016. Phase change material based cold thermal energy storage: materials, techniques and applications – a review. Int. J. Refrigeration 67, 271–289.

Wakili, K.G., Bundi, R., Binder, B., 2004. Effective thermal conductivity of vacuum insulation panels. Build. Res. Inf. 32, 293–299.